Plasmodium Induces Swelling-activated ClC-2 Anion Channels in the Host Erythrocyte*

Stephan M. Huber‡§, Christophe Duranton‡, Guido Henke‡, Claudia van de Sand¶,
Volker Heussler¶, Ekaterina Shumilina‡, Ciprian D. Sandu‡, Valerie Tanneur‡, Verena Brand‡,
Ravi S. Kasinathan‡, Karl S. Lang‡, Peter G. Kremsner‖, Christian A. Hübner**, Marco B. Rust**,
Karin Dedek**‡‡, Thomas J. Jentsch**, and Florian Lang‡

*From the Departments of ‡Physiology and ‖Parasitology, Institute of Tropical Medicine, University of Tübingen, 72076
Germany, the ¶Bernhard Nocht Institute and the **Center for Molecular Neurobiology, University of Hamburg, 20359
and 20251 Germany, and the ‡‡Department of Neurobiology, University of Oldenburg, 26111 Germany*

Intraerythrocytic growth of the human malaria parasite *Plasmodium falciparum* depends on delivery of nutrients. Moreover, infection challenges cell volume constancy of the host erythrocyte requiring enhanced activity of cell volume regulatory mechanisms. Patch clamp recording demonstrated inwardly and outwardly rectifying anion channels in infected but not in control erythrocytes. The molecular identity of those channels remained elusive. We show here for one channel type that voltage dependence, cell volume sensitivity, and activation by oxidation are identical to ClC-2. Moreover, Western blots and FACS analysis showed protein and functional ClC-2 expression in human erythrocytes and erythrocytes from wild type (*Clcn2*$^{+/+}$) but not from *Clcn2*$^{-/-}$ mice. Finally, patch clamp recording revealed activation of volume-sensitive inwardly rectifying channels in *Plasmodium berghei*-infected *Clcn2*$^{+/+}$ but not *Clcn2*$^{-/-}$ erythrocytes. Erythrocytes from infected mice of both genotypes differed in cell volume and inhibition of ClC-2 by ZnCl₂ (1 mM) induced an increase of cell volume only in parasitized *Clcn2*$^{+/+}$ erythrocytes. Lack of ClC-2 did not inhibit *P. berghei* development *in vivo* nor substantially affect the mortality of infected mice. In conclusion, activation of host ClC-2 channels participates in the altered permeability of *Plasmodium*-infected erythrocytes but is not required for intraerythrocytic parasite survival.

Plasmodium falciparum is metabolically highly active and thus depends on ample supply of nutrients (1). In addition, the intraerythrocytic proliferation of the pathogen and the generation of waste products impose a severe challenge to volume constancy of the host red blood cell (RBC)[1] (1). Moreover, the parasite impairs the pump leak balance of the host (2–7), which maintains a high cytosolic K⁺ and a low Na⁺ concentration in non-infected RBCs (8). From 15 and 36 h postinvasion, the K⁺ and Na⁺ leakage through the RBC membrane increases and the Na⁺/K⁺ pump activity decreases, respectively. Both processes result in a replacement of cytosolic K⁺ ions by Na⁺ in the late trophozoite/shizont-infected RBC (6). The parasite requires high Na⁺ and low K⁺ concentrations in the host cytosol (9) most probably to build up inwardly directed Na⁺ and outwardly directed K⁺ gradients across its plasma membrane. However, high cytosolic Na⁺ concentrations lead to cell swelling and eventually to colloidosmotic hemolysis of the host RBC. Premature hemolysis is prevented by the concerted action of the parasite and the host RBC. The former lowers the colloid concentration by excess hemoglobin digestion and the latter exports the hemoglobin-derived amino acids out of the cell (7). To meet the requirements of the intraerythrocytic parasite development new transport systems are up-regulated in the host membrane which accomplish parasite nutrition, cation leakage, and maintenance of host volume constancy (1, 10).

Tracer flux and isosmotic hemolysis experiments characterize the transport systems activated by the parasite as organic osmolyte and anion channels (with additional low but significant cation permeability) (1, 10) similar to those mediating regulatory volume decrease in many nucleated cells (11). Comparison of the available data on the parasite-induced transport suggests that infection of erythrocytes activates two classes of channels, anion-selective channels and organic osmolytes (and cation) channels (12). Recent whole cell patch clamp recordings revealed inwardly rectifying (13–16) and outwardly rectifying anion channels (14, 17, 18) as well as nonselective cation channels (19) in the cell membrane of infected erythrocytes confirming that more than one channel type contributes to the enhanced erythrocyte permeability. The outward rectifier is additionally permeable for organic osmolytes whereas a cell swelling-activated fraction of the inward rectifying anion channels is not (20).

Virtually identical inwardly and outwardly rectifying anion channels are observed in non-infected RBCs following oxidation (14). As *P. falciparum* is known to confer oxidative stress to the host cell (21–25), we hypothesized that *P. falciparum* generates the anion channels by oxidation of endogenous host cell membrane proteins (14). The nature and physiological significance of channel types identified by patch clamp recording, however, have remained a matter of discussion (26, 27). The aim of the present study was to elucidate the molecular identity of one of the infection-induced anion channels and to test for its functional significance for the cell volume maintenance of the infected host RBC.

§ To whom correspondence should be addressed: Dept. of Physiology I, Eberhard-Karls-University Tübingen, Gmelinstrasse 5, D-72076 Tübingen, Germany. Tel.: 49-7071-29-76737; Fax: 49-7071-29-3073; E-mail: stephan.huber@uni-tuebingen.de.

[1] The abbreviations used are: RBC, red blood cell; PBS, phosphate-buffered saline; FACS, fluorescent-activated cell sorter.

EXPERIMENTAL PROCEDURES

Parasites—*P. berghei* ANKA-parasitized mouse RBCs (2×10^6) were injected intraperitoneally into sex- and age-matched wild type (C57BL/6) and ClC-2 knockout mice ($Clcn2^{-/-}$) (28) and parasitemia was determined daily by Syto-16 staining in FACS analysis (see below). For patch clamp experiments, *P. berghei*-infected mouse RBCs were stored in RPMI 1640 medium. The human pathogen *P. falciparum* strains BINH (29) and FCR-3 (30) were grown *in vitro* in banked human RBCs (blood group O+). Parasites were cultured as described earlier (14) at a hematocrit of 5% and a parasitemia of 2–10% in RPMI 1640 medium supplemented with Albumax II (0.5%; Invitrogen) in an atmosphere of 90% N_2, 5% CO_2, 5% O_2.

Patch Clamp—Whole cell currents were recorded at room temperature in late trophozoite stage-infected and non-infected human and mouse RBCs according to Huber *et al.* (14) with solutions buffered to pH 7.4. RBCs were bathed in (in mM:) 115 NaCl, 10 $MgCl_2$, 5 $CaCl_2$ 20 Hepes/NaOH, a solution which was originally designed by Desai *et al.* (13) and which improves the sealing of the cells. Upon achievement of whole cell recording mode, cells were superfused with the recording solutions. After each measurement, cells and Petri dishes were replaced. In whole cell experiments, cytosolic and extracellular ion concentrations are defined by the bath and pipette solution. Electrochemical driving forces result exclusively from the concentration difference of a permeable ion between both bath and pipette solutions and the applied voltage. An osmotic gradient across the recorded membrane to induce cell swelling was generated by either decreasing bath osmolarity (Fig. 1, *A*–*E*) or increasing pipette osmolarity (Figs. 1, *F*–*I*; 4, 5). Human RBCs were recorded with pipette solutions containing (in mM) 140 Na-X, 10 HEPES/NaOH, 5 $MgCl_2$, 1 Mg-ATP, 0.5 EGTA (with X as chloride or D-gluconate) combined with a bath solution of 100 sorbitol, 90 NaCl, 10 HEPES/NaOH, 1 $CaCl_2$, 1 $MgCl_2$. Cell swelling and shrinkage in Fig. 1, *A*–*E* was induced iso-ionically by decreasing and increasing the bath sorbitol to 0 and 250 mM, respectively. Further human RBCs (Fig. 1, *F*–*I*) as well as non-infected and parasitized mouse RBCs (Figs. 4 and 5) were recorded in a bath solution containing (in mM) 140 NMDG-Cl, 10 HEPES/NMDG, 1 $MgCl_2$, 1 $CaCl_2$ in combination with an isotonic (140 mM NMDG-Cl; Fig. 4, *D*–*F*, *closed symbols/bars* and Fig. 5*E*, *closed triangles*) or a hypertonic (170 mM NMDG-Cl; Fig. 4, *A*–*C* and *D*–*F*, *open symbols/bars*, *G* and Fig. 5, *A*–*D* and *E*, *open symbols*) pipette solution (additionally containing in mM: 10 HEPES/NMDG, 0.5 EGTA, 1 $MgCl_2$, 1 Mg-ATP). The hypertonic pipette solution induced cell swelling during recording. Cell shrinkage (Fig. 4*B*, *3rd trace*) and further cell swelling (Fig. 4*B*, *4th trace*) was applied by adding 500 mM sorbitol to the NMDG-Cl bath solution and by diluting the bath solution 1:1.5 with water (95 mM NMDG-Cl), respectively. The ClC-2 inhibitor $ZnCl_2$ was added to the bath solution at concentrations of 0.01–10 mM, the anion channel blocker NPPB (5-nitro-2-3-phenyl-propylamino)-benzoic acid at a concentration of 100 μM. Currents were evoked by 10 voltage pulses (400 ms each) from holding potential (-10 or -30 mV) to voltages between -100 mV and $+80$ mV using 20 mV increments. Currents were analyzed by averaging the whole-cell currents between 350 and 375 ms of each voltage square pulse. Inward conductances were calculated by linear regression of inward current between -60 and 0 mV voltage.

Two Electrode Voltage Clamp—Rat ClC-2 cRNA (31) (25 ng) or water were injected in *Xenopus laevis* oocytes, and currents were recorded by two electrode voltage clamp 3–4 days after injection as has been described in detail elsewhere (32). To study dependence of rClC-2 on cell volume, oocytes were either recorded in isotonic solution containing (in mM) 100 sucrose, 48 NaCl, 5 HEPES/NaOH (pH 7.4), 2 KCl, 1.8 $CaCl_2$, 1 $MgCl_2$ or during cell swelling upon removal of sucrose from the superfusate. For investigating the dependence of rClC-2 on the redox state oocytes were recorded in a solution containing (in mM) 96 NaCl, 2 KCl, 1.8 $CaCl_2$, 1 $MgCl_2$, 5 HEPES/NaOH (pH 7.4). For oxidation and reduction *tert*-butylhydroperoxide (*t*-BHP; 1 mM) and dithiothreitol (5 mM) were added to the superfusate, respectively. Zn^{2+} sensitivity was assessed by adding 0.01–1 mM $ZnCl_2$ to the bath solution.

Density Distribution Assay—Venous blood was drawn retro-orbitally from wild-type and $Clcn2^{-/-}$ mice with heparinized hematocrit capillaries and collected in EDTA-coated tubes to prevent coagulation. Density distribution was obtained according to Danon and Marikovky (33) by using phthalate esters (mixtures of methyl phthalate and di-η-butyl phthalate) in microhematocrit capillaries.

Osmotic Resistance—Venous mouse blood was drawn retro-orbitally and collected in one-fourth volume of 4.3% (w/v) sodium citrate. Citrate-blood (20 μl) was incubated for 2 h in H_2O or in NaCl solutions with different NaCl concentrations ranging from 0.3–0.7% (w/v) NaCl. He-

molysis was quantified photometrically using total hemolysis in H_2O as a reference.

Hematological Parameters—Venous mouse blood was drawn retro-orbitally with heparinized hematocrit capillaries and collected in EDTA-coated tubes. Hematological parameters were determined automatically using Advia 120 Hematology System (Bayer, Germany).

FACS Analysis—To test for oxidation-induced ClC-2 activation (Fig. 3*D*) venous mouse blood was drawn retro-orbitally with heparinized hematocrit capillaries diluted 1:20 in phosphate-buffered saline (PBS) and stored at 4 °C. Mouse RBCs were equilibrated for 15 min at room temperature in 80 mM KCl, 50 mM NaCl, 10 mM HEPES/NaOH (pH 7.4), 4 μM gramicidin D, 2 μM valinomycin, and 50 μM NPPB in the presence or absence of *t*-BHP (1 mM). Cell shrinkage was induced by adding 9 volumes of hypotonic sorbitol solution (200 mM sorbitol, 5 mM HEPES/NaOH (pH 7.4), 4 μM gramicidin D, 2 μM valinomycin, 50 μM NPPB), and the decrease in cell volume was estimated every 60 s by forward scatter in FACS analysis. To test for activation of ClC-2 by *P. berghei* Anka infection (Fig. 3*E*), heparinized blood was taken from malaria-infected $Clcn2^{-/-}$ and wild-type mice with high parasitemia ($70 \pm 6\%$ and $79 \pm 7\%$ in wild type and $Clcn2^{-/-}$, respectively). RBCs were equilibrated for 15 min at room temperature in 125 mM NaCl, 32 mM HEPES/NaOH (pH 7.4), 5 mM KCl, 5 mM D-glucose, 1 mM $MgCl_2$, 1 mM $CaCl_2$, 4 μM gramicidin. Cell shrinkage was induced by adding 9 volumes of 290 mM sorbitol, 5 mM HEPES/NaOH (pH 7.4), 5 mM D-glucose, 4 μM gramicidin D, 100 μM NPPB, and cell volume was determined as described. To determine infection-induced changes in RBC forward scatter (Fig. 6*A*), heparinized blood was taken from *P. berghei*-infected wild-type and $Clcn2^{-/-}$ mice and diluted in RPMI 1640 medium. Cells were further diluted 1:20 in PBS containing the DNA fluorescent dye Syto-16 (3 μM; Molecular Probes, Leiden, The Netherlands) and stained for 40 min. In further experiments studying the effect of $ZnCl_2$ on cell volume (Fig. 6*B*), heparinized, and washed blood from *P. berghei*-infected wild type and $Clcn2^{-/-}$ mice was incubated for 4 h at 37 °C in 125 mM NaCl, 32 mM HEPES/NaOH (pH 7.4), 5 mM KCl, 5 mM D-glucose, 1 mM $MgCl_2$, 1 mM $CaCl_2$, and diluted in the same buffer containing Syto-16 (3 μM). Incubation and Syto-16 staining (40 min) was performed in the presence of $ZnCl_2$ (1 mM) or (for control) of additional $MgCl_2$ (1 mM). Cell volume of Syto-16-positive and -negative cells was analyzed by FACS forward scatter.

Erythrocyte Cell Membrane Preparation and Western Blot—Heparinized blood (from healthy donors; donors gave informed consent) and from wild-type and $Clcn2^{-/-}$ mice was washed (buffy coat was removed) and kept 5–6 days in PBS at 4 °C to eliminate the remaining white blood cells. Thereafter, RBCs were washed in PBS, centrifuged, and the pellet (20 μl) was osmotically hemolyzed in 8 ml of 20 mM HEPES/NaOH (pH 7.4) containing a mixture of protease inhibitors (Roche Applied Science). Ghost membranes were pelleted (15,000 × *g* for 20 min at 4 °C) and lysed in (mM) 125 NaCl, 25 HEPES/NaOH (pH 7.3), 10 EDTA, 10 sodium pyrophosphate, 10 NaF, 0.1% SDS, 0.5% deoxycholic acid, 1% Triton X-100, 10 μl of β-mercaptoethanol. Lysates were separated by 8% SDS-PAGE (50 μg of protein per lane), and blotted to nitrocellulose membranes. Blots were probed overnight at 4 °C with polyclonal rabbit anti-ClC-2 (28) antibody raised against the C-terminal mouse/rat peptide HGLPREGTPSDSDDKCQ (1:600 dilution).

RESULTS

To test for *P. falciparum*-induced activation of cell volume-sensitive ion channels in the host membrane whole cell currents of non-infected and *P. falciparum*-infected human RBCs were recorded in isosmotic, hyposmotic, and hyperosmotic bathing medium. The comparison of Fig. 1, *A* and *B* (*left traces*) clearly demonstrates activation of whole cell currents in the human RBC membrane following infection with *P. falciparum*. As illustrated in Fig. 1*B* (*middle* and *right*) osmotic cell shrinkage inhibited and osmotic cell swelling activated a fraction of the whole cell inward current. The volume-sensitive current fraction amounts to almost 50% of the total inward current in swollen infected cells (Fig. 1*D*). In sharp contrast to the infected RBC, swelling of non-infected human RBCs did not activate any appreciable current (Fig. 1, *A* and *D*, *left two columns*). This indicates that infection is a prerequisite for the activation of the current fraction by cell swelling.

The cell volume sensitive current fraction of infected RBCs activated time-dependently upon hyperpolarization (Fig. 1*C*) and exhibited an inwardly rectifying current voltage (I/V) re-
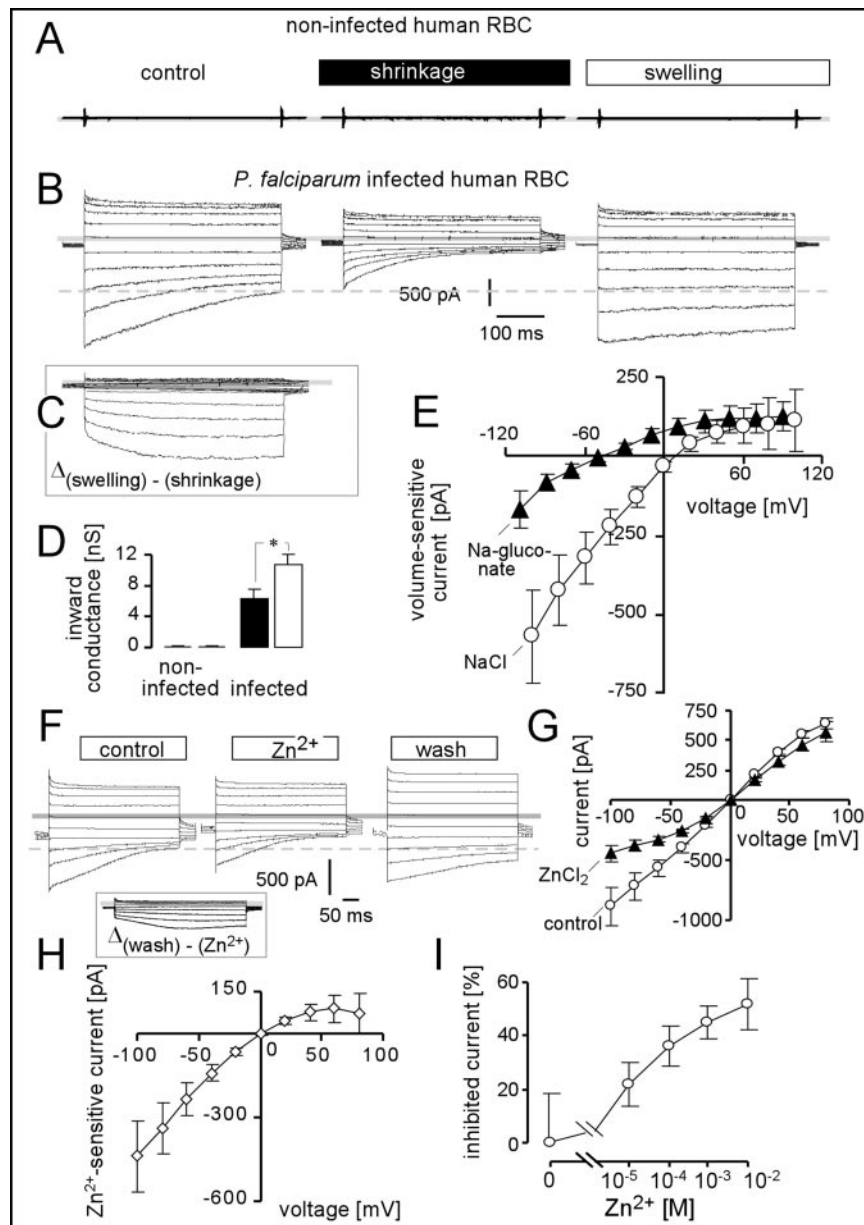
FIG. 1. *P. falciparum* **induces cell volume-sensitive anion channels in human RBCs.** *A* and *B*, whole cell current traces recorded (*A*) in a non-infected and (*B*) in a late trophozoite-infected human RBC in isotonic (control, *left*), hypertonic (shrinkage, *middle*), and hypotonic (swelling, *right*) NaCl bath solution combined with NaCl pipette solution. Currents were evoked by 10 voltage pulses (400 ms each) from −10 mV holding potential to voltages between −100 mV and +80 mV. Applied voltages refer to the cytoplasmic face of the membrane with respect to the extracellular space. Inward currents, defined as entry of positive charge from the extracellular space into the cytosol, are negative currents and depicted as downward deflections of the original current traces. Zero current is indicated by *gray line*. *C*, volume sensitive current fraction as calculated by subtracting the current traces in *B* obtained during cell shrinkage from those during cell swelling. *D*, mean conductance of inward current (as calculated by linear regression between −60 and 0 mV voltage) of non-infected and late trophozoite-infected human RBCs recorded as in (*A* and *B*) with hypertonic (*closed bars*) and hypotonic bath solution (*open bars*). *E*, current-voltage (I/V) relationships of the volume-sensitive current fraction in infected human RBCs recorded as in *B* with NaCl (*open circles*) and sodium D-gluconate pipette solution (*closed triangles*). Data in *D* and *E* were analyzed by averaging the whole cell currents between 350 and 375 ms of each square pulse and depicted as means ± S.E. (n = 5–11; *, $p < 0.05$; two-tailed Student's t test). *F* and *G*, inhibition of cell swelling-induced whole cell currents by $ZnCl_2$ in infected human RBCs. Current traces (*F*) and I/V curves (*G*) recorded in the absence (*left* and *right traces* in *F*, *open circles* in *G*) and presence of $ZnCl_2$ (1 mM; *middle traces* in *F*; *closed triangles* in *G*). Continuous cell swelling was induced by combining a hypertonic pipette solution (170 mM NMDG-Cl) with an isotonic bath solution (140 mM NMDG-Cl). The current traces in the *inset* of *F* show the Zn^{2+}-sensitive current fraction as calculated by subtracting the currents in *F* obtained during Zn^{2+} application from those obtained upon washout. *H*, I/V curve of the $ZnCl_2$-sensitive current fraction as calculated from the data in *G*. *I*, $ZnCl_2$ dose response curve of the whole cell inward current of infected human RBCs during cell swelling (data are means ± S.E.; n = 3–7).

lationship (Fig. 1*E*, *open circles*). Replacement of Cl⁻ in the pipette solution by gluconate in unpaired experiments (Fig. 1*E*, *closed triangles*) demonstrated the anion selectivity of this volume-sensitive current fraction. Addition of $ZnCl_2$ (1 mM) to the bath solution partially inhibited the current of swollen infected human RBCs (Fig. 1, *F* and *G*). The $ZnCl_2$-sensitive current fraction of swollen infected cells activated time-dependently at

hyperpolarizing voltages (Fig. 1*F*, *inset*) and amounted to about 50% of the inward current (Fig. 1*G*). This current fraction (Fig. 1*H*) displayed an inward rectification and absolute current values similar to the swelling-activated fraction (Fig. 1*E*, *open circles*). $ZnCl_2$ inhibited the total inward current of swollen infected cells with an IC_{50} in the range of 100 μM (Fig. 1*I*).

The voltage dependence and the inhibition by Zn^{2+} (34) of

the swelling-induced inwardly rectifying anion current fraction in *P. falciparum*-infected human RBCs resembled that of the ubiquitously expressed, swelling activated Cl^- channel ClC-2 (28, 31, 35–37). If the inwardly rectifying infection-induced anion conductance was indeed generated by ClC-2 then heterologously expressed ClC-2 channels should be activated by oxidative stress. In order to test for sensitivity of ClC-2 to oxidation, we injected mRNA encoding ClC-2 into *Xenopus laevis* oocytes as described previously (35). Two electrode voltage clamp demonstrated volume sensitive and inwardly rectifying anion currents in *Xenopus* oocytes expressing ClC-2 but not in water-injected oocytes (Fig. 2*A*). Exposure of the ClC-2 expressing oocytes to the oxidant *tert*-butylhydroperoxide (*t*-BHP, 1 mM) resulted in a strong activation of inwardly rectifying anion currents (Fig. 2, *B* and *C*), which was reversed upon reduction by dithiothreitol (5 mM; Fig. 2, *B* and *C*). No similar current was induced by oxidation in water-injected oocytes (Fig. 2*C*) indicating that the current was indeed due to activation of ClC-2. The heterologously expressed ClC-2 current was reversibly inhibited by $ZnCl_2$ added to the bath solution with an apparent IC_{50} in the range of about 30 μM (Fig. 2*D*). Those experiments allow us to suggest that, if ClC-2 is expressed in RBCs, it will be activated by oxidative stress imposed by either infection with *P. falciparum* or exposure to oxidants.

Western blot analysis of RBC membrane preparations shows that ClC-2 protein is indeed expressed in erythrocytes. As illustrated in Fig. 3*A*, staining with a ClC-2-specific antibody yielded a single band in human RBCs and two bands in mouse RBCs at the expected molecular size in the range of 100 kDa. The bands were absent in RBCs from $Clcn2^{-/-}$ mice (Fig. 3*A*) confirming the specificity of the antibody.

To test for functional significance of ClC-2 in non-treated mouse RBCs, erythrocyte count, hematocrit, hemoglobin concentration, mean corpuscular volume, mean corpuscular hemoglobin amount, mean corpuscular hemoglobin concentration; and percentage of reticulocytes were measured in non-treated blood from non-infected wild-type and $Clcn2^{-/-}$ mice. In addition, density of non-treated and non-infected mouse RBCs was assessed by the distribution of the RBCs between water and oil mixtures of different densities. Moreover, osmoresistance was measured in these erythrocytes by hemolysis in solutions with decreasing NaCl concentrations. The data indicate that hematological parameters (Table I), cell density (Fig. 3*B*) and osmoresistance (Fig. 3*C*) of RBCs from $Clcn2^{-/-}$ animals did not differ from those of wild-type mice. Thus, ClC-2 did not exert any appreciable physiological function on untreated mouse RBCs.

To test for functional expression of ClC-2, the cation permeability was increased in mouse RBCs by addition of the ionophores valinomycin (2 μM) and gramicidin A (4 μM), and the cells were bathed in a high KCl solution to maintain a high cytosolic K^+ concentration. The subsequent dilution of the medium by KCl-free hypotonic sorbitol solution imposed a strong KCl gradient leading to cellular KCl loss and cell shrinkage. Due to the high cation permeability of the cell membrane the rate of cell shrinkage depended only on anion channel activity. Initial cell swelling in hypotonic sorbitol solution and hyperpolarization of the cation-selective cell membrane are expected to activate putative ClC-2 channels. Inwardly and outwardly rectifying anion channels of infected RBCs differ in NPPB sensitivity (14). Therefore, the experiments were performed in the presence of NPPB at a concentra-tion (50 μM) which should be sufficient to block the outwardly rectifying anion conductance (see Fig. 5*C*) but which should not inhibit ClC-2-like currents in mouse erythrocytes (38). Under those experimental conditions, RBCs from wild-type and $Clcn2^{-/-}$ mice swelled and started to re-adjust their volume
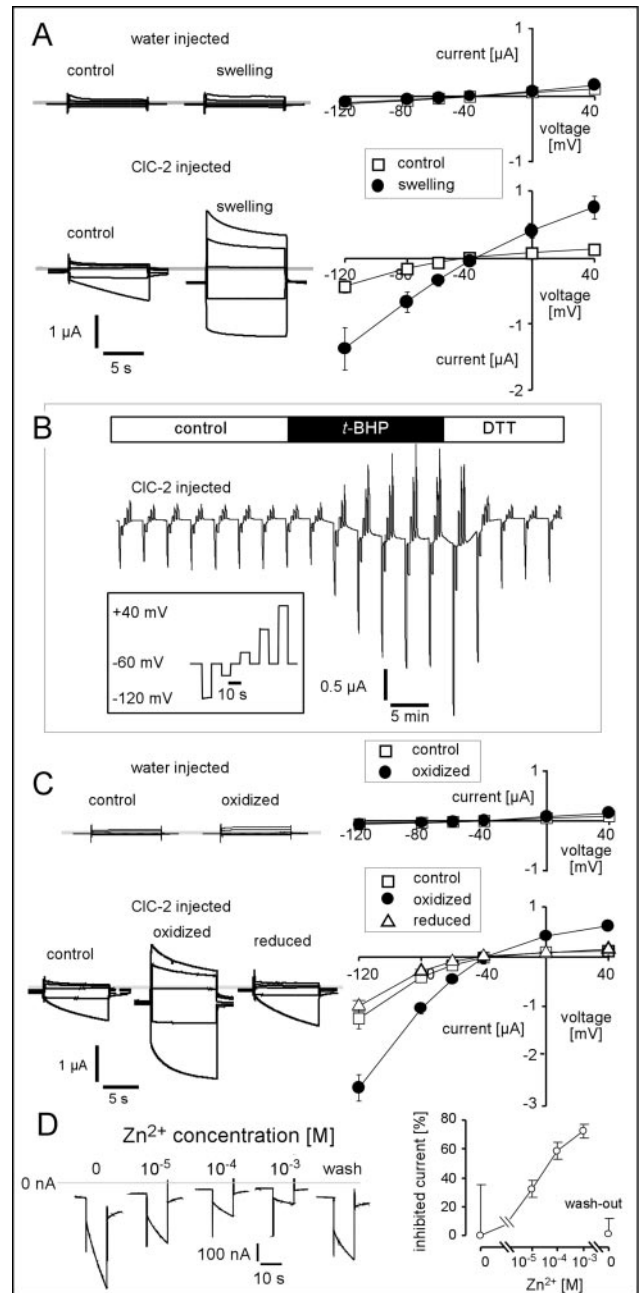
FIG. 2. **Activation of rClC-2 channels heterologously expressed in X. laevis oocytes by cell swelling and by oxidation.** *A*, activation of rClC-2 by exposure to hypotonic bath. *Left*, two electrode voltage clamp traces of a water-injected oocyte (*upper panel*) and a rClC-2-expressing cells (*lower panel*) recorded under isotonic (control) and hypotonic conditions (swelling). Currents were evoked by applying square pulses (10 s each) from −60 mV holding potential to voltages between −120 mV and +40 mV as shown in *B* (*inset*). *Right*, resulting mean I/V relations (±S.E.) of water-injected (*upper plot*; n = 4) and rClC-2-injected oocytes (*lower plot*; n = 24) bathed in isotonic (*open squares*) and hypotonic solution (*closed circles*). *B*, time course of current change of an rClC-2-expressing oocyte subsequently submitted to oxidation (*t*-BHP; 1 mM) and reduction (dithiothreitol; 5 mM). Shown is a current trace at −60 mV holding potential and during applied voltage pulses (pulse protocol is depicted in the *inset*). *C*, activation of rClC-2 by oxidation. *Left*, current traces and, *right*, corresponding mean I/V-curves (±S.E.) from water-injected (*upper panel*; n = 4) and rClC-2-injected oocytes (*lower panel*; n = 24) recorded under control conditions (*left traces*; *open squares*), upon oxidation (*right and middle traces*, respectively; *closed circles*) and upon reduction (*right traces*; *open triangles*). Experimental conditions are as in *B*. *D*, $ZnCl_2$ sensitivity of rClC-2. *Left*, original traces recorded in a rClC-2-injected oocyte in the presence of increasing concentrations of $ZnCl_2$. Currents were obtained at −60 mV holding potential and during a voltage square pulse to −120 mV; *right*, dose response curve as calculated from the data in *D* (means ± S.E., n = 9–15).
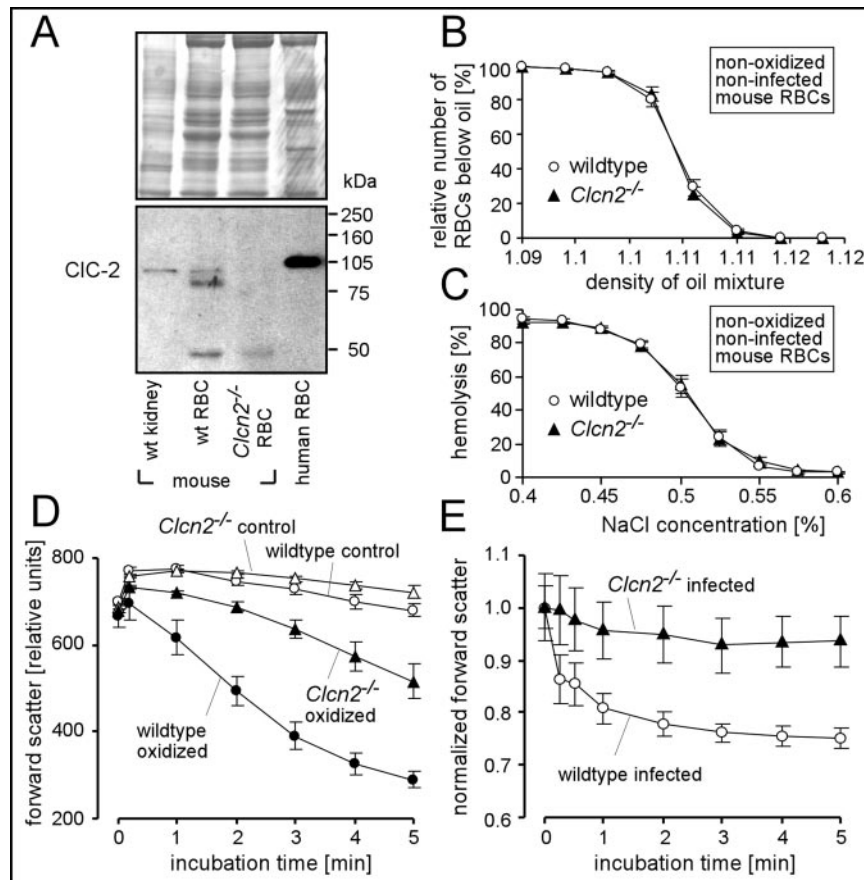
FIG. 3. **Protein and functional expression of ClC-2 in RBCs.** *A*, protein (*upper blot*) and ClC-2 immunostaining (*lower blot*) of membrane preparations from human RBCs, mouse wild-type RBCs, and mouse $Clcn2^{-/-}$ RBCs. Total protein extract from wild-type mouse kidney served as positive control. *B*, density distribution of RBCs from Clcn2$^{-/-}$ (*closed triangles*) and wild-type mice (*open circles*; means ± S.E.; $n = 10$). Distributions were obtained in microhematocrit capillaries by the use of phthalate esters according to Danon and Marikovsky (33). *C*, hemolysis of non-treated mouse RBCs of $Clcn2^{-/-}$ (*closed triangles*) and of wild-type mice (*open circles*; means ± S.E.; $n = 10$) suspended in decreasing concentrations of NaCl (means ± S.E.; $n = 10$). *D*, oxidation-induced cell-shrinkage of cation-permeabilized RBCs. Shown are cell-volume changes upon suspension of KCl-equilibrated mouse RBCs in K$^+$- and Cl$^-$-free solution containing the chloride channel blocker NPPB (50 μM). This maneuver induced cell shrinkage by loss of cell KCl and water, which was dependent mainly on a NPPB-insensitive Cl$^-$ conductance. Mean forward scatter (±S.E. of $n = 4$ mice in each group) was determined by FACS analysis as a measure of cell volume. Data are given for control (*open symbols*) and oxidized (*t*-BHP, 1 mM for 15 min; *closed symbols*) RBCs taken from wild-type (*circles*) and $Clcn2^{-/-}$ mice (*triangles*). *E*, shrinkage of cation-permeabilized mouse RBCs infected with *P. berghei* Anka. Time course of changes in forward scatter (means ± S.E.; $n = 6$) upon resuspension of NaCl-equilibrated parasitized mRBC in Na$^+$- and Cl$^-$-free solution containing NPPB (100 μM). Forward scatters were normalized to the respective initial (0 min) values. RBCs were drawn from malaria-infected wild-type and $Clcn2^{-/-}$ mice with high parasitemia.

within 5 min of incubation in hypotonic sorbitol solution (Fig. 3*D*, *open symbols*) as measured by changes of forward scatter in FACS analysis. This regulatory volume decrease was significantly ($p \leq 0.05$; two-tailed Welch-corrected *t* test) more pronounced in wild type than in $Clcn2^{-/-}$ RBCs (slope of forward scatter decrease: -20 ± 6 *versus* -6 ± 2 rel. units/min in wild type and $Clcn2^{-/-}$ RBCs, respectively; $n = 4$) suggesting low basal ClC-2 activity prior to oxidation. Following oxidative stress (addition of 1 mM *t*-BHP for 15 min) the same maneuver led to rapid shrinkage of RBCs, which was significantly ($p \leq 0.01$; two-tailed Welch-corrected *t* test) faster in RBCs from wild-type mice than from $Clcn2^{-/-}$ mice (slope of forward scatter decrease: -110 ± 15 *versus* -35 ± 8 rel. units/min in oxidized wild-type and oxidized $Clcn2^{-/-}$ RBCs, respectively; $n = 4$; Fig. 3*D*, *closed symbols*). Thus, ClC-2 is functionally expressed and activated by oxidative stress in mouse RBCs. The observed slow shrinkage of oxidized $Clcn2^{-/-}$ RBCs (Fig. 3*D*, *closed triangles*) may be due to residual activity of non-ClC-2 anion conductances similarly activated by oxidation but not fully blocked by NPPB (50 μM). Therefore a higher concentration of NPPB (100 μM) was used in the following experiments.

Late trophozoite-infected RBCs have high cytosolic Na$^+$ and

TABLE I
Hematological parameters of wild-type and Clcn2$^{-/-}$ mice

		Erys[a]	Hb[b]	Hct[c]	MCV[d]	MCH[e]	MCHC[f]	Reti[g]
		$\times 10^6/\mu l$	g/dl	%	fl	pg	g/dl	%
Wild type	Mean	9.74	15.38	47.53	48.81	15.80	32.44	3.88
($n = 15$)	S.E.	0.10	0.24	0.63	0.54	0.19	0.63	0.34
$Clcn2^{-/-}$	Mean	9.68	15.19	47.34	48.89	15.72	32.22	4.50
($n = 14$)	S.E.	0.20	0.29	1.46	0.99	0.15	0.66	0.32

[a] Erys, erythrocyte count.
[b] Hb, hemoglobin concentration.
[c] Hct, hematocrit.
[d] MCV, mean corpuscular volume.
[e] MCH, mean corpuscular hemoglobin.
[f] MCHC, mean corpuscular hemoglobin concentration.
[g] Reti, percentage of reticulocytes.

low cytosolic K$^+$ concentrations (2–7). To test for ClC-2 activation by *P. berghei*-infection Na$^+$-permeabilized mRBCs from malaria-infected wild-type and $Clcn2^{-/-}$ mice (>70% parasitemia) were resuspended in isosmotic sorbitol solution, and cell shrinkage was assessed by FACS forward scatter in the presence of NPPB (100 μM). Fig. 3*E* shows that $Clcn2^{-/-}$ deficiency significantly ($p \leq 0.001$; two-tailed Welch-corrected *t* test) de-

FIG. 4. **ClC-2-dependent inwardly rectifying anion currents in mouse RBC.** *A–C*, whole cell current traces recorded at different time points (as indicated) in a non-infected wild-type (*A*), a *P. berghei*- (late trophozoite)-infected wild-type (*B*), and an infected *Clcn2$^{-/-}$* mouse RBC (*C*). Continuous cell swelling was induced by combining a hypertonic pipette solution (170 mM NMDG-Cl) with an isotonic bath solution (140 mM NMDG-Cl). In addition, in *B* cell shrinkage and further strong cell swelling was evoked by increasing and decreasing the bath osmolarity by 450 and 150 mosM, respectively. *D* and *E*, I/V relations recorded as in *B* and *C* with hypertonic pipette solution (170 mM NMDG-Cl; *open circles*) and isotonic bath solution (swollen) were compared with those obtained in unpaired experiments with isotonic pipette (140 mM NMDG-Cl; *closed triangles*) and bath solution (non-swollen). Data are means ± S.E. (*n* = 11–26) from infected RBC of wild-type (*D*) and *Clcn2$^{-/-}$* mice (*E*). *F*, mean conductances (±S.E.) of the inward current as calculated from the data in *D* and *E* by linear regression between −60 mV and 0 mV voltage. ***, $p < 0.001$; two-tailed Student's *t* test). *G*, mean I/V curve (±S.E.; *n* = 3) of the cell volume-sensitive current fraction ($\Delta I = I_{\text{strong swelling}} - I_{\text{shrinkage}}$; see *B*) in infected wild-type mouse-RBCs. The *inset* displays the calculated tracing of ΔI.
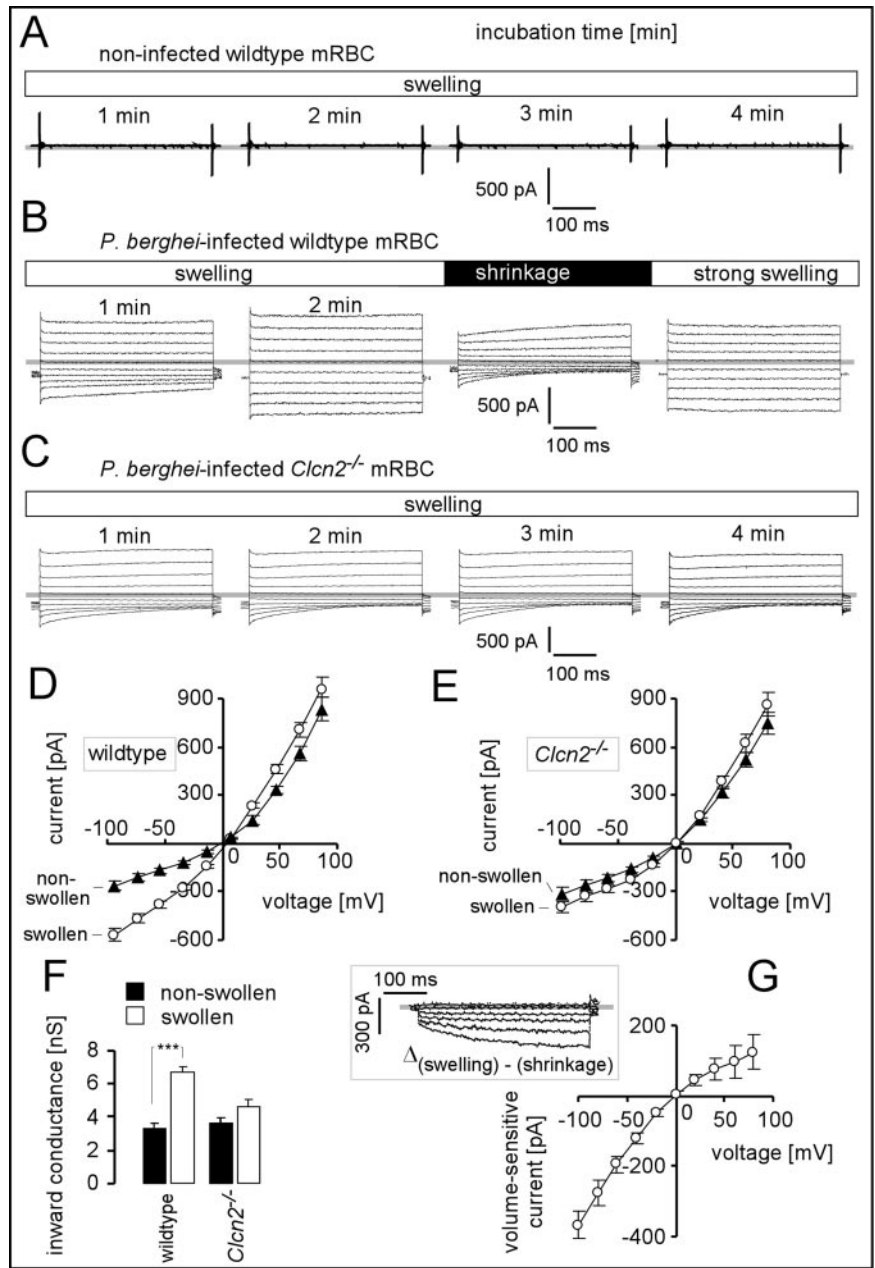
creased the slope of forward scatter decline (−87 ± 12 *versus* −28 ± 6 rel. units/min in wild-type and *Clcn2$^{-/-}$* RBCs, respectively; *n* = 3–6) indicating infection-induced activation of ClC-2.

To directly test for activation of ClC-2 channels by *Plasmodium* infection, patch clamp whole cell recordings were performed in *P. berghei*-infected RBCs from wild-type and *Clcn2$^{-/-}$* mice. *In vivo* infected mouse RBCs exhibited whole cell currents which resembled those of infected human RBCs in anion selectivity, current amplitude, rectification, and time-dependent in-/activation at strong hyper-/depolarizing voltages (compare Fig. 4*B*, *third trace* with Fig. 1*B*, *second trace*). In analogy to human RBCs, cell swelling activated and cell shrinkage inactivated an anion current fraction in infected but not in non-infected RBCs from wild-type mice (Fig. 4, *A* and *B*). In sharp contrast, no cell volume-sensitive current fraction was measurable in infected RBCs from *Clcn2$^{-/-}$* mice (Fig. 4, *C*, *E*, and *F*). The current phenotype of infected *Clcn2$^{-/-}$* RBCs was identical to that of infected wild-type RBCs during cell shrink-

age (compare Fig. 4, *C* with *B*, *third traces* or 5*A*, *first traces*) indicating similar expression of the infection-induced non-ClC-2 anion conductances by both genotypes. Comparison of the I/V curves recorded in both genotypes under control conditions (Fig. 4, *D* and *E*; *closed triangles*) and during cell swelling (Fig. 4, *D* and *E*; *open circles*) revealed a ClC-2-dependent inwardly rectifying current fraction which amounted to about 3 nS (Fig. 4*G*). It contributed about 50% of the inward current in swollen cells (Fig. 4*D*) similar to the volume sensitive inward current fraction of infected human RBCs (Fig. 1*D*). The phenotype of the ClC-2 current in infected mouse RBCs (Fig. 4*G*) did not differ from the infection-induced, volume sensitive, and inwardly rectifying anion conductance of human RBCs (Fig. 1, *C* and *E*) and ClC-2 channels heterologously expressed in *Xenopus laevis* oocytes (Fig. 2) in rectification behavior and slow activation at hyperpolarizing voltages. ZnCl$_2$ (1 mM) and NPPB (100 μM) added to the bath inhibited the whole cell currents of swollen RBCs from wild-type mice additively (Fig. 5, *A–C*) suggesting that NPPB (100 μM) had only a minor effect on the

FIG. 5. **Zn^{2+} sensitivity of the ClC-2 currents in *P. berghei*-infected mouse RBCs.** Effect of ZnCl$_2$ (1 mM), NPPB (100 μM), or NPPB/ZnCl$_2$ (100 μM/1 mM) on the currents in infected wild-type-RBCs during cell swelling (170 mM NMDG-Cl-pipette/140 mM NMDG-Cl bath). *A*, original traces recorded at different time periods upon reaching whole cell recording configuration (at time −1 min). *B* and *C*, mean I/V curves (±S.E.; *n* = 5–6) recorded as in (*A*; 5 min values) in the absence (control) and presence of ZnCl$_2$ (1 mM; *B*) or NPPB (100 μM; *C*), respectively. *D*, dependence of the inward current on the ZnCl$_2$ concentration. Records were obtained as in *A* from infected wild-type mRBCs during cell swelling. ZnCl$_2$ dose response curve of whole cell inward current in swollen wild-type mouse-RBC (means ± S.E.; *n* = 4–8 and means, *n* = 2 for 0–1 mM and 10 mM Zn^{2+}, respectively). *E*, Zn^{2+} (1 mM)-sensitive current fraction (means ± S.E.) of infected swollen RBCs (170 mM NMDG-Cl pipette/140 mM NMDG-Cl bath) from wild-type (*open circles*; *n* = 6) and *Clcn2$^{-/-}$* mice (*open diamonds*; *n* = 7) and of infected non-swollen wild-type RBCs (*closed triangles*; 140 mM NMDG-Cl pipette/140 mM NMDG-Cl-bath; *n* = 3).
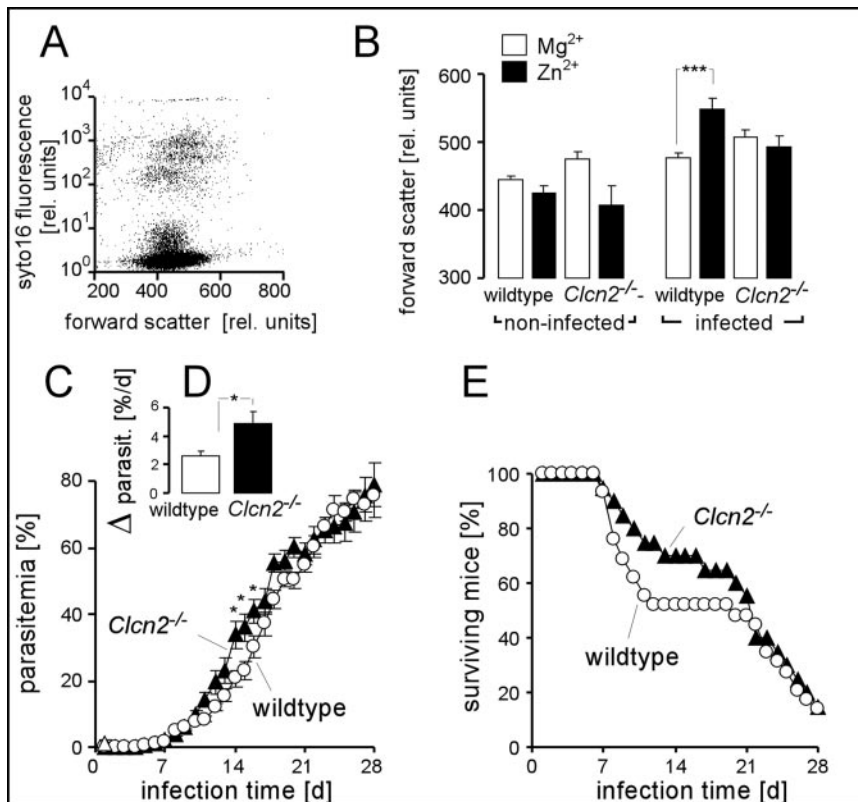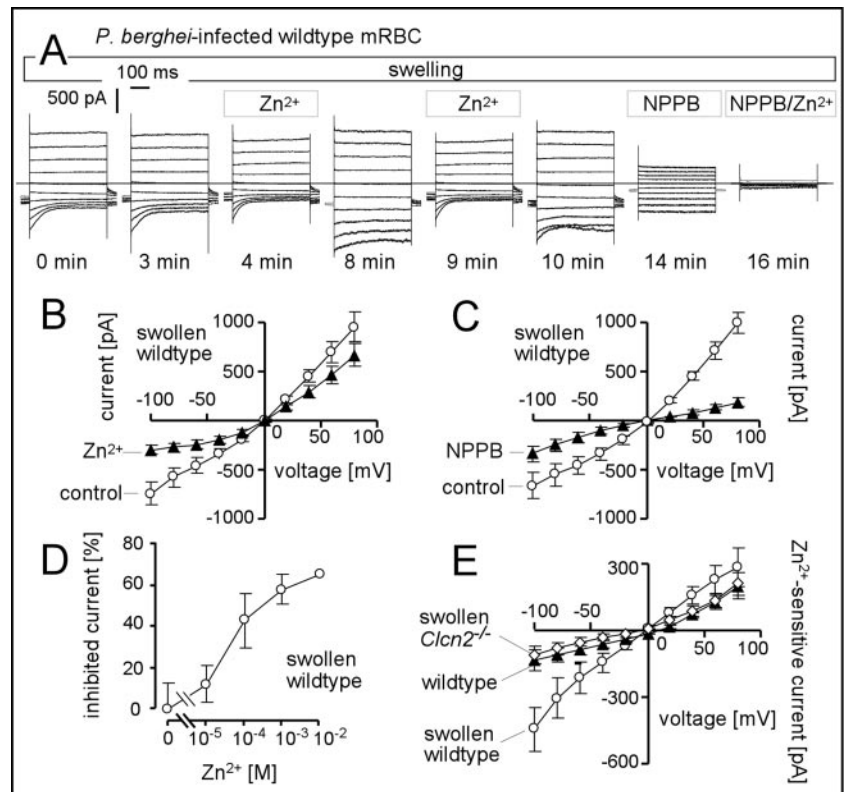

FIG. 6. **Functional significance of the Zn^{2+}-sensitive ClC-2-dependent anion channels in *P. berghei*-infected mRBCs.** *A*, dot blot recorded by FACS showing fluorescence intensity of the DNA-specific dye syto16 against forward scatter of RBCs from infected mice (individual sample). *B*, forward scatter reflecting cell volume (mean ± S.E.) of non-infected (*i.e.* syto16-negative) and *P. berghei*-infected (*i.e.* syto16-positive) RBCs from wild-type (*n* = 17) and *Clcn2$^{-/-}$* mice (*n* = 10). Forward scatter was recorded in mRBCs post-incubated for 4 h at 37 °C in the presence of ZnCl$_2$ or MgCl$_2$ (1 mM each). *C*, time course of mean parasitemia (±S.E.) in *P. berghei* Anka-infected *Clcn2$^{-/-}$* mice (*closed triangles*; *n* = 20) and their wild-type littermates (open circles; *n* = 29; *, *p* ≤ 0.05; two-tailed Student's *t* test). *D*, mean parasitemia increase (±S.E.) in infected *Clcn2$^{-/-}$* (*closed bar*; *n* = 14) and wild-type mice (*open bar*; *n* = 15) as calculated from *C* by linear regression between day 8 and 14 of infection. *, *p* ≤ 0.05; two-tailed Student's *t* test. *E*, survival of *P. berghei* Anka-infected *Clcn2$^{-/-}$* and wild-type mice (same experiments as in *C*).

ZnCl$_2$-sensitive current fraction but inhibited the ZnCl$_2$-insensitive outwardly rectifying current fraction almost completely. ZnCl$_2$ inhibited the total inward current of swollen RBCs from wild-type mice with an IC$_{50}$ in the range of 100 μM (Fig. 5*D*). Comparison of the ZnCl$_2$ (1 mM)-sensitive current fraction between whole cell currents of swollen wild-type (Fig. 5*E*, *open circles*), swollen *Clcn2$^{-/-}$* RBC (Fig. 5*E*, *open diamonds*) and

non-swollen wild-type RBCs (Fig. 5*E*, *closed triangles*) indicated Zn^{2+}-sensitivity of the cell volume sensitive ClC-2-generated current fraction.

The swelling-induced activation of ClC-2 points to a possible role of this channel in regulatory volume decrease of swollen RBCs. Thus, ClC-2 deficiency may impair cell volume regulation of infected RBCs leading to an increase in host cell volume.

To test this possibility, RBCs freshly drawn from *P. berghei*-infected $Clcn2^{-/-}$ and wild-type mice were stained with the DNA/RNA fluorescence dye Syto 16 and analyzed by FACS. (Fig. 6*A*). Because mature mouse and human RBCs are devoid of nuclei, mitochondria, and RNA, this staining allows to differentiate between non-infected (*i.e.* Syto 16-negative) and parasitized RBCs (*i.e.* Syto 16 positive). Both, non-infected and parasitized cells from infected $Clcn2^{-/-}$ mice, exhibited a significantly ($p \leq 0.05$, one-way analysis of variance) higher forward scatter (488 ± 7 and 515 ± 10 rel. units, $n = 20$, respectively) than the corresponding wild-type RBC groups (457 ± 6 and 481 ± 7 rel. units, $n = 16$, respectively). As *P. berghei* amplifies in an asynchronous manner in mice (39) all stages are encountered at a particular time point and differences in cell volume, therefore, cannot be attributed to difference in stages of parasite development (6). Thus, the observed differences in forward scatter suggest an enhanced RBC volume induced by *Clcn2* deficiency. In further experiments, the effect of ClC-2 inhibition on forward scatter was determined in non-infected and parasitized RBCs from both genotypes. Incubation with $ZnCl_2$ (1 mM for 4 h at 37 °C) induced a significant increase in forward scatter of parasitized wild-type RBCs but not of non-infected wild type or non-infected and parasitized $Clcn2^{-/-}$ RBCs (Fig. 6*B*). Thus inhibition of ClC-2 increased cell volume only in parasitized RBCs.

To test for the functional significance of ClC-2 for the malaria infection *in vivo*, $Clcn2^{-/-}$ mice and their wild-type littermates (20–29 mice each) were infected with *P. berghei* Anka (2×10^6 parasitized RBCs intraperitoneally) and increase in parasitemia and animal survival monitored. Infection was followed by increasing parasitemia in both genotypes with similar time courses (albeit parasites initially developed somewhat faster in $Clcn2^{-/-}$ mice; Fig. 6, *C* and *D*). Some of the wild-type littermates tended to die slightly earlier than $Clcn2^{-/-}$ mice after infection with *P. berghei* Anka, but $Clcn2^{-/-}$ mice and their wild-type littermates eventually approached similar survival rates. Taken together, lack of ClC-2 did not prevent infection with *P. berghei* Anka and had no profound influence on the course of the disease in mice.

DISCUSSION

The present observations provide conclusive evidence for expression of ClC-2 channels in RBCs and show that the channels are activated by oxidation and by infection with *Plasmodium*. The present study thus confirms the participation of host cell membrane proteins in the altered permeability of infected erythrocytes. The data further disclose the functional significance of ClC-2 in cell volume maintenance of infected host cells. Inhibition of ClC-2 resulted in a cell volume increase in infected RBCs, suggesting that Cl^- efflux via inorganic monovalent anion-selective channels contributes to regulatory volume decrease of the infected cells.

A prerequisite for anion channel-generated Cl^- efflux during regulatory volume decrease is a membrane potential more negative than Cl^- equilibrium potential. This occurs for instance in dying human RBCs when increased free cytosolic Ca^{2+} concentrations stimulate the activation of Gardos K^+ channels (40). Consequently, human RBCs hyperpolarize toward K^+ equilibrium potential. Hyperpolarization in turn imposes an outwardly directed driving force for Cl^- leading to channel-mediated efflux of K^+, Cl^-, and osmotically obliged H_2O, and RBC shrinkage.

Parasitized RBCs, reportedly, do not activate Gardos K^+ channels (41) due to only moderate Ca^{2+} leakage through the host membrane (42), unimpaired Ca^{2+} ATPase activity of the host RBC (43), and Ca^{2+} uptake by the parasite (44, 45), which together prevent an increase of the cytosolic-free Ca^{2+} concentration in the host cytosol. The infection-induced permeabilities, however, have themselves a low but significant permeability for monovalent inorganic cations, which probably is generated by a Ca^{2+}-permeable cation channel type different from the anion channels (19). This cation permeability exhibits a K^+-to-Na^+ permeability ratio of about 2 (6, 19, 46). Therefore, the activity of the cation permeability should drive Cl^- out of the cell (because the loss of K^+ is expected to exceed the uptake of Na^+) especially in the first phase of trophozoite development when the Na^+ pump activity maintains high outwardly directed K^+- and inwardly directed Na^+ gradients across the host membrane (6, 19, 46). In this infection stage net loss of monovalent cations together with Cl^- counteracts the expansion of the host volume by the parasite metabolisms. Accordingly, cell volume of infected RBCs was increased upon inhibition of ClC-2 channels.

Besides ClC-2 at least two further anion channel types have been demonstrated in *P. falciparum*-infected human erythrocytes. An outwardly rectifying channel type, which exhibits an additional permeability for organic osmolytes such as lactate, sorbitol, and mannitol (20) and an inwardly rectifying channel type (13, 15, 16). The latter has been reported to be dependent on CFTR (16) and to be activated in non-infected human RBCs by membrane stretch, by protein kinase A phosphorylation (47), and by hypertonic shrinkage (16) indicating that this channel type is also generated by host proteins. The pharmacology of this inwardly rectifying anion channel resemble those determined with tracer flux and isosmotic hemolysis in *P. falciparum*-infected human RBCs suggesting an organic osmolyte permeability also for this inwardly rectifying anion channel (13, 15). More recently, this function has been challenged by the observation that parasites develop well in RBCs from cystic fibrosis patients (mutations in both CFTR alleles), *i.e.* in the absence of these inwardly rectifying anion channels (16). Nevertheless, there might be considerable functional redundancy of inwardly and outwardly rectifying (putative) organic osmolyte and anion channels. Moreover, whether a principally inwardly or outwardly rectifying current phenotype is measurable in *P. falciparum*-infected human RBCs strongly depends on the applied experimental patch-clamp protocol suggesting that parasitized RBCs can recruit the (putative) organic osmolyte and anion channel types in dependence on extracellular signals (serum factors) or membrane potential (18). In contrast to these (putative) osmolyte channels, the swelling-induced inwardly rectifying anion conductance of *P. falciparum*-infected human RBCs is reportedly not permeable to organic osmolytes (20) indicating that channels other than ClC-2 account for the hemolysis of *Plasmodium*-infected RBCs in isosmotic solutions of organic osmolytes.

A further result of the present study is that *P. berghei* Anka infection *in vivo* induced inwardly and outwardly rectifying anion channels in the mouse RBC membrane very similar to those observed in human RBC infected *in vitro* with *P. falciparum*. Reportedly, RBCs from mice infected with *P. vinckei* increase the rate of furosemide-sensitive choline, taurine, and Rb^+ influx (48). As in *P. falciparum*-infected human RBCs (1), the infection-induced choline uptake is dependent on the counter anion in the medium and occurs via a nonsaturable pathway. Taken together these data strongly suggest that *Plasmodium* infection induces similar changes in erythrocyte membrane permeability in mouse and man.

Functionally, *P. falciparum*-infected human RBCs resemble many nucleated cell types which accomplish regulatory volume decrease by the concerted action of ClC-2 channels and organic osmolyte and anion channels (11, 49). The present study demonstrates that both, ClC-2 and the organic osmolyte and anion

ClC-2 in Parasitized Erythrocytes

channels, are contributing to cell volume constancy of the parasitized RBC. Swelling-dependent ClC-2 activity might sense changes in RBC volume and might fine tune cell volume of parasitized RBCs (especially during early infection) while the cell volume-independent activity (20) of the organic osmolyte and anion channels might generate the constitutive efflux of chloride and organic osmolytes (lactate and hemoglobin-derived amino acids). The observed function of ClC-2 on cell volume did not limit the intraerythrocyte amplification of *Plasmodium in vivo* since *P. berghei* Anka developed well in $Clcn2^{-/-}$ mice. Thus the organic osmolyte and anion channels or other channels up-regulated by the *Clcn2* deficiency may functionally replace ClC-2.

Non-infected human RBCs, in sharp contrast, do not utilize anion channels for regulatory volume decrease (50). Accordingly, in the present study ClC-2 currents were not activated in non-infected human and mouse RBCs during cell-swelling and only low ClC-2 activity was apparent in non-infected cells from FACS forward scatter experiments (Fig. 3*D*). Similar to infection, oxidation potentiated the activation of ClC-2 channels by cell swelling suggesting that oxidative processes are triggering ClC-2 activity also in infected cells. Oxidation also activated heterologously expressed ClC-2 in *Xenopus* oocytes indicating that the underlying signaling is not confined to the RBC. In *Xenopus* oocytes oxidation-induced activation of ClC-2 was reversed by reducing agents. Similarly, *P. falciparum*-induced activation of both anion channel types in human RBCs is fully reversed following addition of reduced glutathione (GSH) into the patch pipette, whereas the addition of oxidized glutathione (GSSG) is without effect (14).

In conclusion, oxidative processes activate ClC-2 anion-selective channels which participate together with organic osmolytes and anion channels in the maintenance of the cell volume of *Plasmodium*-infected erythrocytes.

REFERENCES

1. Kirk, K. (2001) *Physiol. Rev.* **81,** 495–537
2. Overman, R. R. (1951) *Physiol. Rev.* **31,** 285–311
3. Dunn, M. J. (1969) *J. Clin. Investig.* **48,** 674–684
4. Ginsburg, H., Handeli, S., Friedman, S., Gorodetsky, R., and Krugliak, M. (1986) *Z. Parasitenkd.* **72,** 185–199
5. Lee, P., Ye, Z., Van Dyke, K., and Kirk, R. G. (1988) *Am. J. Trop. Med. Hyg.* **39,** 157–165
6. Staines, H. M., Ellory, J. C., and Kirk, K. (2001) *Am. J. Physiol. Cell. Physiol.* **280,** C1576–1587
7. Lew, V. L., Tiffert, T., and Ginsburg, H. (2003) *Blood* **101,** 4189–4194
8. Tosteson, D. C., and Hoffman, J. F. (1960) *J. Gen. Physiol.* **44,** 169–194
9. Brand, V. B., Sandu, C. D., Duranton, C., Tanneur, V., Lang, K. S., Huber, S. M., and Lang, F. (2003) *Cell. Physiol. Biochem.* **13,** 347–356
10. Ginsburg, H., and Kirk, K. (1998) in *Malaria: Parasite Biology, Pathogenesis, and Protection* (Sherman, I. W., ed), pp. 219–232, A.S.F. Microbiology, Washington, D. C.
11. Kirk, K., and Strange, K. (1998) *Annu. Rev. Physiol.* **60,** 719–739
12. Ginsburg, H., and Stein, W. D. (2004) *J. Membr. Biol.* **197,** 113–134
13. Desai, S. A., Bezrukov, S. M., and Zimmerberg, J. (2000) *Nature* **406,** 1001–1005
14. Huber, S. M., Uhlemann, A. C., Gamper, N. L., Duranton, C., Kremsner, P. G., and Lang, F. (2002) *EMBO J.* **21,** 22–30
15. Egee, S., Lapaix, F., Decherf, G., Staines, H. M., Ellory, J. C., C., D., and Thomas, S. L. Y. (2002) *J. Physiol.* **542,** 795–801
16. Verloo, P., Kocken, C. H., Van der Wel, A., Tilly, B. C., Hogema, B. M., Sinaasappel, M., Thomas, A. W., and De Jonge, H. R. (2004) *J. Biol. Chem.* **279,** 10316–10322
17. Baumeister, S., Endermann, T., Charpian, S., Nyalwidhe, J., Duranton, C., Huber, S., Kirk, K., Lang, F., and Lingelbach, K. (2003) *Mol. Biochem. Parasitol.* **132,** 35–45
18. Staines, H. M., Powell, T., Ellory, J. C., Egee, S., Lapaix, F., Decherf, G., Thomas, S. L., Duranton, C., Lang, F., and Huber, S. M. (2003) *J. Physiol.* **552,** 177–183
19. Duranton, C., Huber, S., Tanneur, V., Lang, K., Brand, V., Sandu, C., and Lang, F. (2003) *Cell. Physiol. Biochem.* **13,** 189–198
20. Duranton, C., Huber, S. M., Tanneur, V., Brand, V. B., Akkaya, C., Shumilina, E. V., Sandu, C. D., and Lang, F. (2004) *J. Gen. Physiol.* **123,** 417–426
21. Atamna, H., and Ginsburg, H. (1993) *Mol. Biochem. Parasitol.* **61,** 231–241
22. Atamna, H., Pascarmona, G., and Ginsburg, H. (1994) *Mol. Biochem. Parasitol.* **67,** 79–89
23. Ginsburg, H., and Atamna, H. (1994) *Parasite* **1,** 5–13
24. Becker, K., Gui, M., Traxler, A., Kirsten, C., and Schirmer, R. H. (1994) *Histochemistry* **102,** 389–395
25. Atamna, H., and Ginsburg, H. (1997) *Eur. J. Biochem.* **250,** 670–679
26. Ginsburg, H. (2002) *Trends Parasit.* **18,** 346
27. Huber, S., Uhlemann, A., Gamper, N., Duranton, C., Lang, F., and Kremsner, P. (2002) *Trends Parasit.* **18,** 346–347
28. Bosl, M. R., Stein, V., Hubner, C., Zdebik, A. A., Jordt, S. E., Mukhopadhyay, A. K., Davidoff, M. S., Holstein, A. F., and Jentsch, T. J. (2001) *EMBO J.* **20,** 1289–1299
29. Binh, V. Q., Luty, A. J., and Kremsner, P. G. (1997) *Am. J. Trop. Med. Hyg.* **57,** 594–600
30. Jensen, J. B., and Trager, W. (1978) *Am. J. Trop. Med. Hyg.* **27,** 743–746
31. Thiemann, A., Grunder, S., Pusch, M., and Jentsch, T. J. (1992) *Nature* **356,** 57–60
32. Wagner, C. A., Friedrich, B., Setiawan, I., Lang, F., and Broer, S. (2000) *Cell. Physiol. Biochem.* **10,** 1–12
33. Danon, D., and Marikovsky, V. (1964) *J. Lab. Clin. Med.* **64,** 668–674
34. Clark, S., Jordt, S. E., Jentsch, T. J., and Mathie, A. (1998) *J. Physiol.* **506,** 665–678
35. Grunder, S., Thiemann, A., Pusch, M., and Jentsch, T. J. (1992) *Nature* **360,** 759–762
36. Jentsch, T. J., Stein, V., Weinreich, F., and Zdebik, A. A. (2002) *Physiol. Rev.* **82,** 503–568
37. Nehrke, K., Arreola, J., Nguyen, H. V., Pilato, J., Richardson, L., Okunade, G., Baggs, R., Shull, G. E., and Melvin, J. E. (2002) *J. Biol. Chem.* **277,** 23604–23611
38. Komwatana, P., Dinudom, A., Young, J. A., and Cook, D. I. (1994) *Pflugers Arch.* **428,** 641–647
39. Biarnais, T., Landau, I., and Richard-Lenoble, D. (2002) *Parasite* **9,** 51–57
40. Lang, P. A., Kaiser, S., Myssina, S., Wieder, T., Lang, F., and Huber, S. M. (2003) *Am. J. Physiol. Cell. Physiol.* **285,** C1553–1560
41. Kirk, K., Elford, B. C., and Ellory, J. C. (1992) *Biochim. Biophys. Acta* **1135,** 8–12
42. Staines, H. M., Chang, W., Ellory, J. C., Tiffert, T., Kirk, K., and Lew, V. L. (1999) *J. Membr. Biol.* **172,** 13–24
43. Tiffert, T., Staines, H. M., Ellory, J. C., and Lew, V. L. (2000) *J. Physiol.* **525,** 125–134
44. Leida, M. N., Mahoney, J. R., and Eaton, J. W. (1981) *Biochem. Biophys. Res. Commun.* **103,** 402–406
45. Tanabe, K., Mikkelsen, R. B., and Wallach, D. F. (1982) *J. Cell Biol.* **93,** 680–684
46. Kirk, K., and Horner, H. A. (1995) *J. Biol. Chem.* **270,** 24270–24275
47. Egee, S., Harvey, B. J., and Thomas, S. (1997) *J. Physiol.* **504,** 57–63
48. Staines, H. M., and Kirk, K. (1998) *Biochem. J.* **334,** 525–530
49. Strange, K., Emma, F., and Jackson, P. S. (1996) *Am. J. Physiol.* **270,** C711–730
50. Cossins, A. R., and Gibson, J. S. (1997) *J. Exp. Biol.* **200,** 343–352

Plasmodium **Induces Swelling-activated ClC-2 Anion Channels in the Host Erythrocyte**

Stephan M. Huber, Christophe Duranton, Guido Henke, Claudia van de Sand, Volker Heussler, Ekaterina Shumilina, Ciprian D. Sandu, Valerie Tanneur, Verena Brand, Ravi S. Kasinathan, Karl S. Lang, Peter G. Kremsner, Christian A. Hübner, Marco B. Rust, Karin Dedek, Thomas J. Jentsch and Florian Lang

Access the most updated version of this article at doi: 10.1074/jbc.M407618200

Alerts:
- When this article is cited
- When a correction for this article is posted

Click here to choose from all of JBC's e-mail alerts